https://doi.org/10.15407/ujpe67.11.765

R. SINGH, R. BALA, S.S. SAMBYAL

Department of Physics, University of Jammu
(Jammu Tawi-180006, India; e-mails: randhir.singh@cern.ch, Renu.Bala@cern.ch, sanjeev.singh.sambyal@cern.ch)

CENTRALITY AND TRANSVERSE SPHEROCITY DEPENDENT STUDY OF CHARGED-PARTICLE PRODUCTION IN Xe–Xe COLLISIONS AT $\sqrt{s_{NN}} = 5.44$ TeV USING PYTHIA8 ANGANTYR AND AMPT MODELS

Transverse spherocity is an event structure variable which provide an effective way to disentangle the data into hard and soft components of the processes corresponding to events with small and large numbers of multiparton interactions (MPI), respectively. Recent experimental results in small systems from the LHC suggest the importance of the transverse spherocity variable in the classification of the events. In this contribution, we have studied the dynamics of identified particle production in Xe–Xe collisions at $\sqrt{s_{NN}} = 5.44$ TeV using A Multi-Phase Transport Model (AMPT) and the recently developed Angantyr model, which is incorporated within PYTHIA8. A study of the transverse momentum spectra of the identified particles is presented for soft (isotropic) and hard (jet-like) events in different centrality intervals.

Keywords: quark-gluon plasma, pseudorapidity, heavy-ion collisions, AMPT, PYTHIA8, Angantyr model.

1. Introduction

The study of the behavior of the matter under extreme conditions of temperature and energy density is important to understand the processes involved in the phase transition of the matter in Quantum Chromodynamics (QCD). Experiments at Relativistic Heavy Ion Collider (RHIC) at BNL, USA and Large Hadron Collider (LHC) at CERN, Geneva, Switzerland are specially designed to study the matter under these extreme conditions. In these experiments, the results have suggested that a strongly interacting de-confined state of quarks and gluons, also called Quark-Gluon Plasma (QGP), is formed in ultra-relativistic heavy-ion collisions. This plasma is a very hot and dense state and exists for a very short duration of time. The relevant degrees of freedom in the QGP phase are quarks and gluons instead of mesons and baryons (which are color neutral confined state). After the formation, this QGP cools, expands hydrodynamically, and reaches firstly the chemical freeze-out (the hadron abundances are fixed) phase and then reaches the kinetic freeze-out (the hadron momenta are fixed) phase.

The observable which is important to cahracterize the properties of the created matter in these collisions is the multiplicity of the charged particles. This is due to the fact that the particle production is affected by the initial energy density reached in the collision. The colliding nuclei are extended objects. Therefore, in a collision, the region of overlap between the two colliding nuclei varies from collision to collision. This degree of overlap is expressed by the impact parameter (denoted as "b"). The impact parameter cannot be measured directly. To overcome

this difficulty, a different parameter called centrality is used. The centrality characterizes the initial overlapping region geometry, which corresponds to the number of participating nucleons $N_{\rm part}$ and binary collisions $N_{\rm coll}$. $N_{\rm part}$ and $N_{\rm coll}$ will be different for similar overlaps in collisions of nuclei of different sizes.

Transverse spherocity is an event shape variable which has been introduced recently. The recent development in event shape variables provides an alternate way to characterize the high multiplicity events in small systems considering particle production, event multiplicity, and event shape variable together. Event shape observables provide information about the energy distribution in an event. The event shape observables calculated event-by-event allows one to isolate jet-like (high p_T jets) and isotropic (partonic scattering with low Q^2) events [1]. The ALICE, CMS, and ATLAS experiments have done the studies based on transverse spherocity [2,3]. These studies involved the understanding of event shape as a function of the charged particle multiplicity of the event. The results from these studies show that, for a high multiplicity, the events are more isotropic. After studying extensively small systems [4], the use of the transverse spherocity parameter in heavy-ion collisions may reveal new and unique results from heavy-ion collisions, where the production of a QGP is well established fact.

Transverse momentum (p_T) spectra of the charged particles produced in the heavy-ion collisions carry the essential information about the thermal nature of the interacting system [5–11]. The Maxwell–Boltzmann distribution law tells us that the p_T spectra are related to the temperature of the system formed in these collisions. At low to intermediate p_T (up to 10 GeV/c), the collective expansion of the system governs the charged particle production, which is observed in the shapes of single-particle transverse-momentum spectra [12, 13] and multiparticle correlations [14]. At high p_T (typically above 10 GeV/c), the parton fragmentation governs the particle production. This production is affected by the amount of energy loss that the partons suffer, when propagating in the medium. Moreover, the numbers of charged particles ($N_{\rm ch}$) produced in these ultra-relativistic collisions are also related to the temperature and energy density of the system created. The ratios of the yields of identified hadrons are also important to understand the processes involved in the production of hadron. The ratios of protons to pions (p/π) and kaons to pions (K/π) characterize the relative baryon and meson productions, respectively.

In this work, we have explored all the above-mentioned aspects related to the particle production. We have also used the transverse spherocity for the first time in Xe–Xe collisions at $\sqrt{s_{NN}} = 5.44$ TeV using A Multi-Phase Transport Model (AMPT) [15] and the Angantyr model [16] which is incorporated in PYTHIA8. The purpose of the present analysis is to study the dynamics of heavy-ion collisions using transverse spherocity and collision centrality in Xe–Xe collisions. Thus, we have used the PYTHIA8 and the string melting parametrization available in the AMPT model. We hope for that this would drive experimentalists to pursue such study in experiments at RHIC and LHC. The work is arranged as follows. We begin with a brief introduction and the motivation for the study in Section 1. In Section 2, the detailed analysis methodology along with a brief description of AMPT and PYTHIA (Angantyr) is given. Section 3 discusses the results for the charged-particle pseudorapidity density, p_T spectra of $\pi^{\pm}$, $K^{\pm}$, and $p^{\pm}$ in different centrality and transverse spherocity ranges. Finally, the results are summarized in Section 4.

2. Event Generation and Analysis Methodology

This section is devoted to discussions related to the event generators, AMPT, and PYTHIA8 (Angantyr). Around 0.5 Million Xe–Xe events have been generated for both event generators at $\sqrt{s_{NN}} = = 5.44$ TeV. A discussion will also be presented for the transverse spherocity.

2.1. PYTHIA8 (Angantyr)

PYTHIA8 is a general-purpose Monte Carlo event generator that has been quite successful in the study of elementary particle collisions. It has been extensively used to simulate proton-proton and proton-lepton collisions to understand the dynamics of strong and electroweak processes extending from high momentum transfer regions (perturbative scales) to the scales around $\Lambda_{\rm QCD}$ (Lattice QCD scales). Recently, efforts have been made to modify PYTHIA8 that

made it possible to simulate ultra-relativistic heavy-ion collisions like proton-nuclei (pA) and nuclei-nuclei (AA) ones. PYTHIA8 incorporates what is called "Angantyr" which basically superpose many pp collisions to make a single heavy-ion collision. In this way, a bridge is formed between heavy ion and high energy hadron phenomenologies. An important point is to note that the assumption of the formation of a hot thermalized medium is not included in the Angantyr model, since the production mechanisms is the same as in small collision systems. Thus, it can be used to differentiate the effects of collective and non-collective behaviors in heavy-ion collisions.

The Angantyr model is basically inspired by the old Fritiof model and the notion of wounded nucleons, but with the inclusion of effects of hard partonic interactions. To calculate the number of wounded nucleons, the use of the Glauber model is made, with the consideration of fluctuations in the nucleon-nucleon (NN) interactions to differentiate non-diffractively and diffractively wounded nucleons. In the model, the fluctuations of the nucleonic wavefunction are accommodated as fluctuations in the nuclei radius. Nucleons inside nuclei are distributed randomly according to a Glauber formalism. Every nucleon is then identified as either wounded or a spectator. The interactions between wounded nucleons in the projectile and target are classified as elastic, non-diffractive (ND), secondary non-diffractive (SND), single-diffractive (SD), and double-diffrative (DD) which basically depends on the interaction probability. All the subevents generated at the parton level are stacked together to represent one pA or AA collision event.

In PYTHIA8, the hadronization is done via the Lund string fragmentation model. In this model, the Lund area law [17] provides the probability of creating hadrons from the initial state of partons. The produced partons are connected to the beam remnants through color fluxtubes or strings which store the potential energy. As the partons move away from each other, the string breaks causing the formation of new quark-antiquark pairs. This process continues until the string pieces reduce to very small pieces, which are recognized as shell hadrons. In this scheme, the reconnection of strings between the partons happens in such a way that the string length decreases; resulting in a decrease in the particle production and, hence, the multiplicity.

2.2. A multiphase transport (AMPT) model

The AMPT model has four main components: the initial conditions, partonic interactions, conversion from the partonic to the hadronic matter, and hadronic interactions. In the case of default AMPT model, initial conditions for heavy ion collisions at RHIC are carried from the HIJING model [18–20]. The production of particles is described either as hard or soft components. The hard components are the ones that involve a momentum transfer larger than a cutoff momentum p_0, while the soft components are the ones having a momentum transfer below the cutoff value. The hard component is evaluated in the perturbative Quantum Chromodynamics domain (pQCD) using parton distribution functions in a nucleus. These processes contribute to the production of the minijets of partons. The soft component is discussed in non-perturbative region and is modeled by the formation of strings. The excited strings then decay independently following the Lund JETSET fragmentation model. The energy density in the default AMPT model can be very high in heavy ion collisions. To incorporate this effect, the AMPT model is extended to include the string melting mechanism. The interactions between partons are described using equations of motion which can be approximately written as the Boltzmann ones. The Boltzmann equations are then solved by using Zhang's parton cascade (ZPC) [21], in which two partons undergo the scattering, whenever they are within the minimum closest distance. In the String Melting version of AMPT (AMPT-SM), colored strings are melted to form low-momentum partons, which takes place at the start of the ZPC. Corresponding to two different initial conditions, the hadronization is also done via two different mechanisms. In the case of default AMPT model, the minijets and their remaining parent nucleons coexist, and, after partonic interactions, they together form new excited strings. The Lund string fragmentation model describes the hadronization of these strings. In the case of the AMPT model with string melting, the conversion of strings into soft partons takes place. Then the hadronization happens via the simple quark coalescence model. In the coalescence model, the hadronization is done by combining three closest quarks (antiquarks) into a baryon (antibaryon) and two closest partons into a meson. The

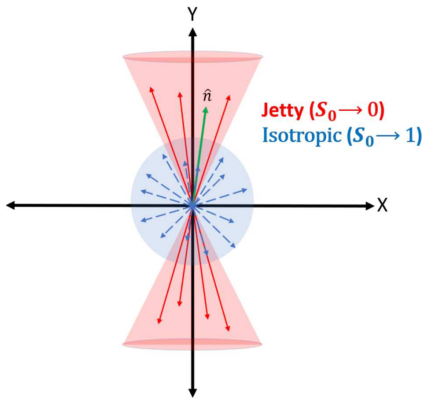

Fig. 1. Jetty and isotropic events in the transverse plane [25]

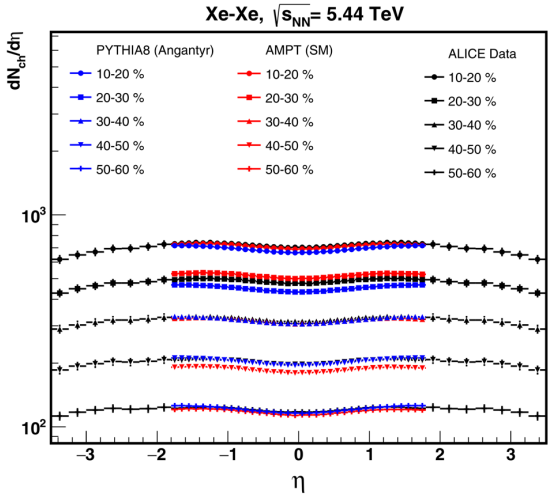

Fig. 2. Charged-particle pseudorapidity density for different centrality classes over a broad η range in Xe–Xe collisions at $\sqrt{s_{NN}} = 5.44$ TeV calculated with AMPT and PYTHIA8. The results are also compared with those from the ALICE experiment at the LHC at CERN

Table 1. **Table showing the values of impact parameter for AMPT and summed transverse energy for PYTHIA8 for different centrality bins**

Centrality, %	AMPT		PYTHIA8	
	$N_{\rm ch}^{\rm min}$	$N_{\rm ch}^{\rm max}$	$E_T^{\rm min}$	$E_T^{\rm max}$
0–10	1685.3	4998.5	1031.47	2000
10–20	1122.7	1685.3	729.13	1031.47
20–30	729.2	1122.7	502.604	729.13
30–40	453.6	729.2	330.139	502.604
40–50	263.7	453.6	202.442	330.139
50–60	140.8	263.7	111.821	202.442
60–70	68.1	140.8	53.8031	111.821

hadrons thus produced undergo the final evolution via the meson-meson, meson-baryon, and baryon-baryon interactions described by the relativistic transport mechanism. The quark coalescence mechanism for the hadronization well explains the spectra at the mid-p_T regions and the particle flow [22–24]. Thus, for our work, we have used the AMPT-SM mode (AMPT version 2.26t7) with the default settings.

2.3. Transverse spherocity

Transverse spherocity (S_0) is the property of an event and is defined using a unit vector $\hat{n}(n_T, 0)$ which minimizes the ratio [26] and chosen from all possible unit transverse vectors:

$$S_0 = \frac{\pi^2}{4} \min_{\hat{n}=(n_x,n_y,n_y)} \left(\frac{\sum_i |\mathbf{p}_{T_i} \times \hat{n}_T|}{\sum_i p_{T_i}} \right)^2. \tag{1}$$

The factor, $\pi^2/4$ normalizes the minimized value to 1 for the isotropic case. As a result, the value of transverse spherocity runs from 0 to 1, as the distribution of particles deviates from the jet-like to an isotropic structure, respectively, i.e.,

$$S_0 = \begin{cases} 0 & \text{pencil-like limit (hard events),} \\ 1 & \text{isotropic limit (soft events).} \end{cases} \tag{2}$$

Figure 1 shows the distribution of particles in both the scenarios.

3. Results

In Fig. 2, the charged-particle multiplicity density $dN_{\rm ch}/d\eta$ as a function of the pseudorapidity for different centrality classes is presented for AMPT and PYTHIA8. The centrality intervals for AMPT are defined using the charged-particle multiplicity distribution as can be seen in Table 1, whereas, for PYTHIA8, we define the centrality intervals which are based on the summed transverse energy (ΣE_T) in the pseudorapidity interval [–0.8, 0.8]. The motivation behind the use of the summed transverse energy distribution to define the centrality intervals has been studied in [16]. Figure 3 shows the distribution of events as a function of the charged-particle multiplicity for the AMPT generator, while Fig. 4 shows the event distribution for the PYTHIA8 event generator as a function of the summed transverse energy (ΣE_T). The $dN_{\rm ch}/d\eta$ values are also compared with the results

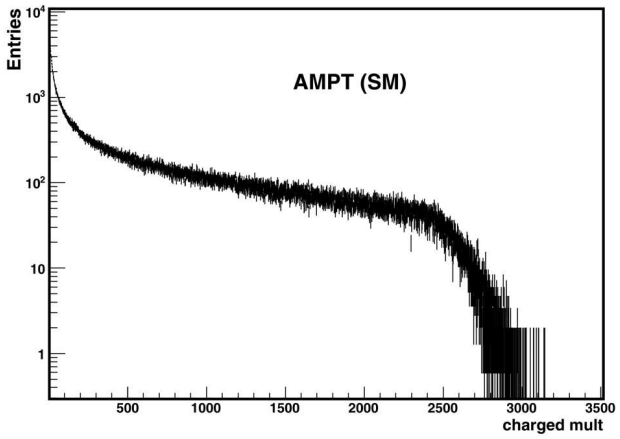

Fig. 3. Event distribution as a function of the charged-particle multiplicity for the AMPT model

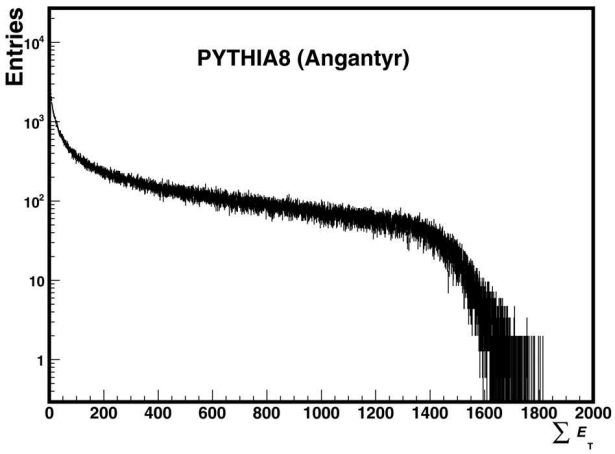

Fig. 4. Event distribution as a function of the summed transverse energy ($\sum E_T$) for the PYTHIA8 Angantyr model

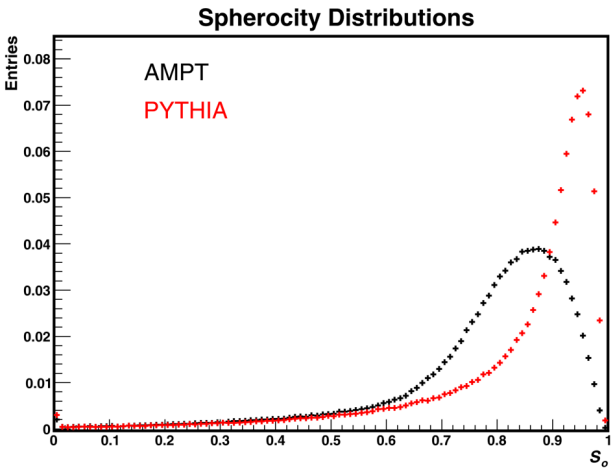

Fig. 5. Event distribution as a function of transverse spherocity in different centrality intervals for the PYTHIA8 Angantyr model

from the experimental study with the ALICE Detector at the LHC at CERN [27]. In ALICE, the centrality classes are defined by using the sum of the amplitudes of the signals in the V0-A and V0-C detectors. The V0 system provides a charged particle multiplicity measurement based on the energy deposited in the scintillators. As mentioned above, Ref. [16] compares the measured V0 amplitude in ALICE with the $\sum E_T$ variable. The shape of the distribution is described quite well and, hence, ΣE_T can be used as a centrality observable.

From Fig. 2, it can be seen that the AMPT describes the data fairly well at low centralities and slightly overestimates at high centralities. On the other hand, PYTHIA8 produces the shape pretty well, but slightly overestimates the data in the small centrality bins. For the Angantyr model, we find that the fluctuations, as well as the distinction between primary and secondary absorption-damaged nucleons, have a fairly significant impact on the final-state multiplicity. It is to be noted that AMPT presumes that a hot dense thermalized medium is formed in which a collective expansion occurs, whereas PYTHIA lacks a mechanism to reproduce the collective effects seen in pp collisions. Therefore, the Angantyr model lacks the assumption of production of a medium as well. Figure 5 shows the transverse spherocity distribution of the events in the 0–100% centrality interval for AMPT (black markers) and PYTHIA8 (red markers). The figure indicates that the more events produced by the PYTHIA8 are isotropic in nature as compared to AMPT. Figures 6 and 7 present the transverse spherocity distribution of events in different centrality classes for AMPT and PYTHIA8, respectively. It can be seen from the figures that small-centrality (high-multiplicity) events are more toward isotropic in nature, whereas high-centrality (low-multiplicity) events are toward the jetty side. This means that the peak of the transverse spherocity distribution shifts toward jetty events with the centrality, which shows that more central events contribute to the softer events and vice versa. The process of isotropization in a many-particle final state occurs through multiple interactions between the quanta of the system. If the final-state multiplicity in

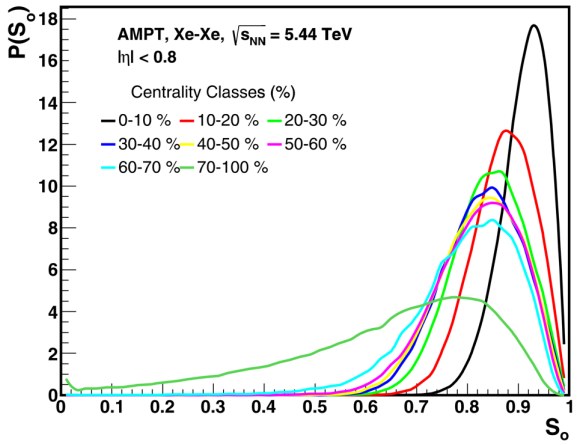

Fig. 6. Event distribution as a function of transverse sphericity in different centrality intervals for the AMPT model

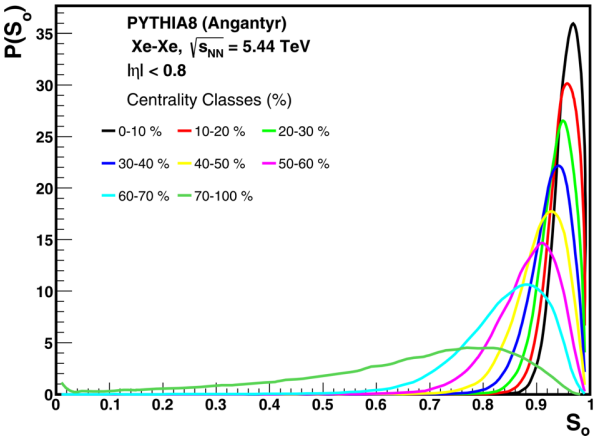

Fig. 7. Event distribution as a function of transverse sphericity in different centrality intervals for the PYTHIA8 Angantyr model

Table 2. **Table showing the values of transverse spherocity for jetty and isotropic ranges for different centrality bins**

Centrality, %	AMPT		PYTHIA8	
	Jetty	Isotropic	Jetty	Isotropic
0–10	0–0.87	0.95–1	0–0.93	0.97–1
10–20	0–0.82	0.92–1	0–0.92	0.96–1
20–30	0–0.78	0.90–1	0–0.91	0.96–1
30–40	0–0.76	0.89–1	0–0.89	0.95–1
40–50	0–0.75	0.89–1	0–0.87	0.94–1
50–60	0–0.74	0.88–1	0–0.83	0.93–1
60–70	0–0.72	0.87–1	0–0.77	0.93–1

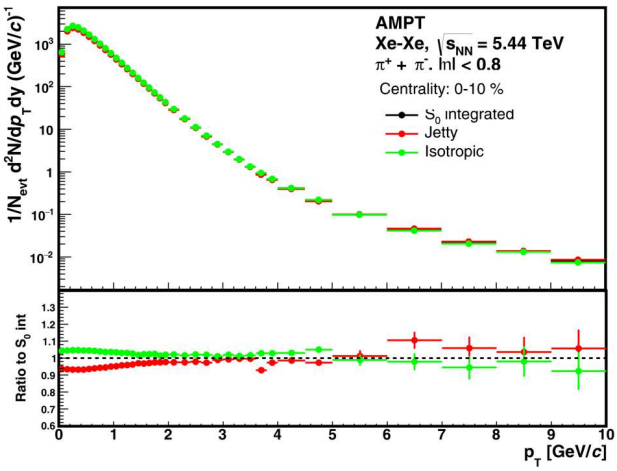

Fig. 8. p_T spectra of $\pi^{\pm}$ in the *centrality* bin 0–10% bin for AMPT

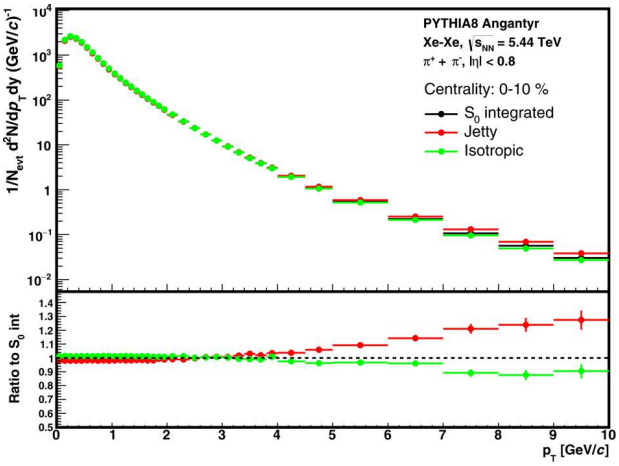

Fig. 9. p_T spectra of $\pi^{\pm}$ in the *centrality* bin 0–10% bin for PYTHIA

an event is higher, the probability of that the event will become isotropic is also higher [7, 28, 29]. Therefore, the differential study of the particle production as a function of the centrality and transverse spherocity classes has great importance to understand the particle production mechanism. As the distribution depends on the centrality and ultimately on the charged-particle multiplicity. Therefore, to define the jetty and isotropic limits of the transverse spherocity, the 20% events of the extremum of the spherocity distribution are considered. The cuts for jetty and isotropic events vary for different centrality classes which are shown in Table. 2.

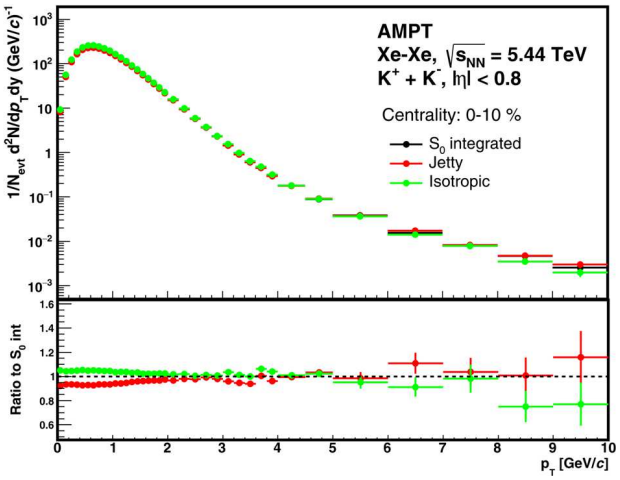

Fig. 10. p_T spectra of $K^{\pm}$ in the *centrality* bin 0–10% bin for AMPT

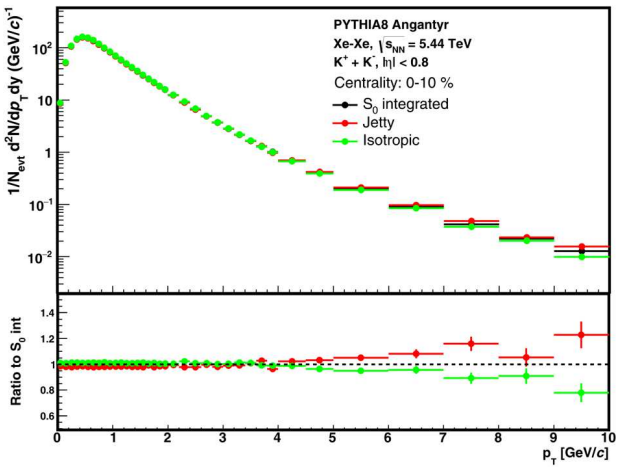

Fig. 11. p_T spectra of $K^{\pm}$ in the *centrality* bin 0–10% bin for PYTHIA

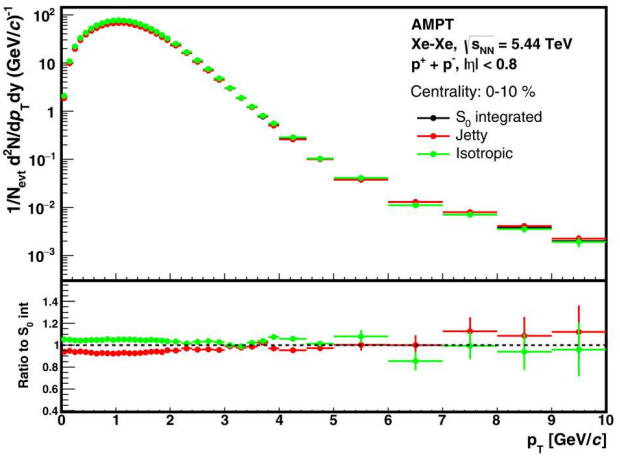

Fig. 12. p_T spectra of $p^{\pm}$ in the *centrality* bin 0–10% bin for AMPT

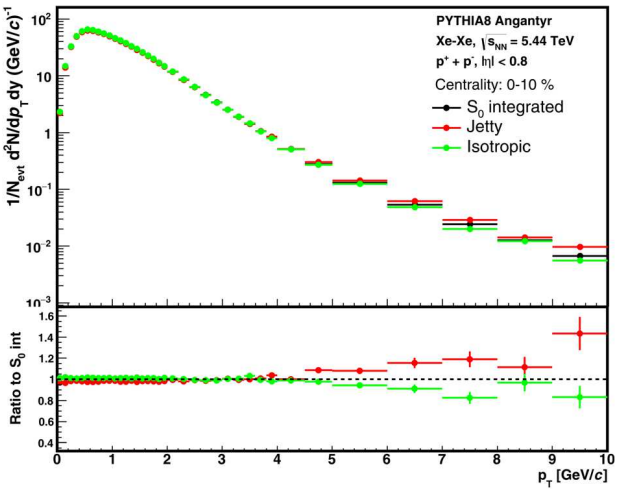

Fig. 13. p_T spectra of $p^{\pm}$ in the *centrality* bin 0–10% bin for PYTHIA

The p_T spectra of particles ($\pi^{\pm}$, $K^{\pm}$ and $p^{\pm}$) have been studied in jetty and isotropic regions of the transverse spherocity for different centrality classes at the mid-rapidity $|\eta| < 0.8$. Figures 8 to 13 represent the transverse spherocity distribution for AMPT and PYTHIA8 generators in the centrality class 0–10%. Similarly, Figs. 14 to 19 represent the p_T spectra in the centrality interval 60–70%. The jetty region of transverse spherocity corresponds to lower 20% of the events in the spherocity distribution, whereas the isotropic region corresponds to higher 20% of the events in the spherocity distribution, and the integrated region is defined over the complete transverse spherocity ($0 \leq S_0 \leq 1$) region. The ratio of the p_T -spectra for isotropic and jetty events with respect to the spherocity integrated events ($0 < S_0 < 1$) is shown in the lower panels. From the figures, we find that the low p_T regions are dominated by isotropic events rather than jetty ones. However, this scenario is reversed, when moving to higher p_T. At certain points called *crossing point*, the jetty event dominates over the isotropic event. Therefore, the study of *crossing points* is of great interest with respect to feasible limits of event-type dominance and, hence, related particle generation mechanisms. As we pass from low to high multiplicities, it has been observed from prior

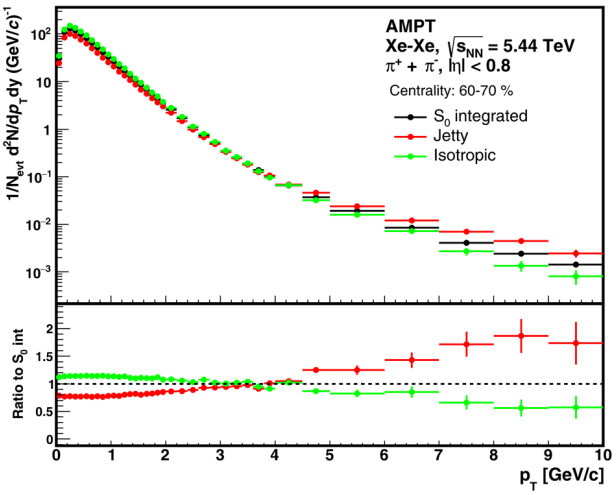

Fig. 14. p_T spectra of $\pi^{\pm}$in the *centrality* bin 60–70% bin for AMPT

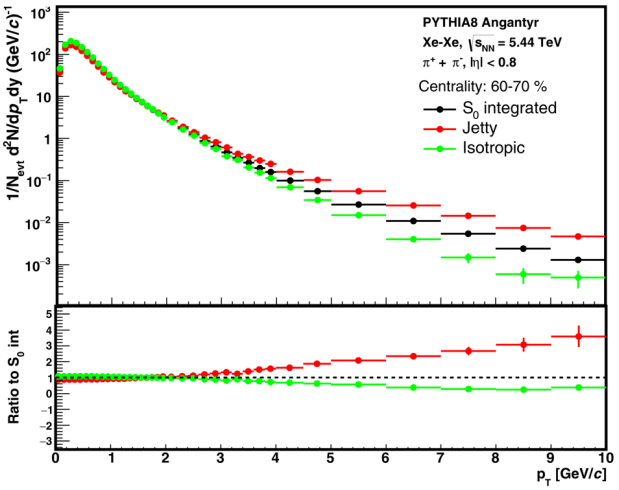

Fig. 15. p_T spectra of $\pi^{\pm}$in the *centrality* bin 60–70% bin for PYTHIA

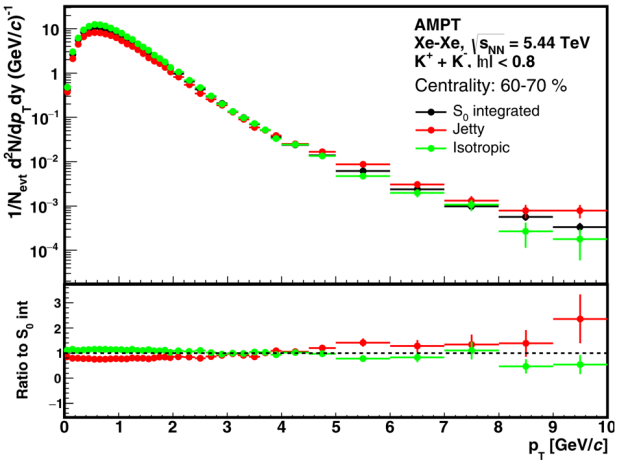

Fig. 16. p_T spectra of $K^{\pm}$ in the *centrality* bin 60–70% bin for AMPT

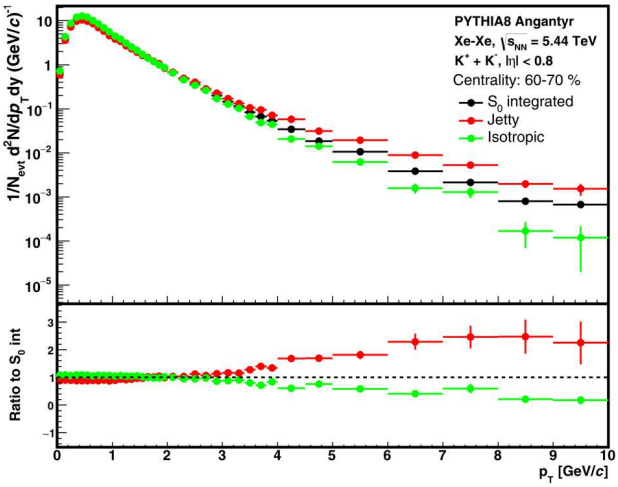

Fig. 17. p_T spectra of $K^{\pm}$ in the *centrality* bin 60–70% bin for PYTHIA

investigations of the light-flavor sector that the *crossing point* relies on the multiplicity greatly and that the isotropic events are populated over numerous events [25, 30, 31]. According to the observations, the QGP-like effects observed in high-multiplicity pp collisions may not be caused by jet-bias effects, but instead may be caused by a potential system development, which should be investigated. In the present work, similar studies of the identified particles ($\pi^{\pm}$, $K^{\pm}$, and $p^{\pm}$) in the central pseudorapidity region $|\eta| < 0.8$ in the heavy-ion collision system show that isotropic events are dominant at low centralities (high-multiplicities) and vice versa. Figure 20 shows the *crossing point* in different centrality ranges for PYTHIA8 and AMPT event generators. The values are also presented in Table 3. This illustrates how, for two event generators, the contribution of jets to the creation of charged particles varies with centrality conditions. From the Table 3 and Fig. 20, a comparison shows a shift of the *crossing point* toward lower-p_T in the case of PYTHIA8 Angantyr model indicating the jet dominant contribution to the particle production for the AMPT model. This means that the contribution of jets is higher in AMPT as compared to PYTHIA8. The dominance of isotropy in low

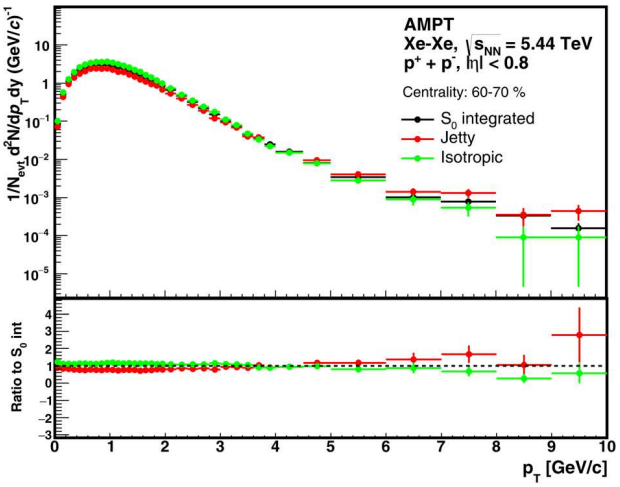

Fig. 18. p_T spectra of $p^{\pm}$ in the *centrality* bin 60–70% bin for AMPT

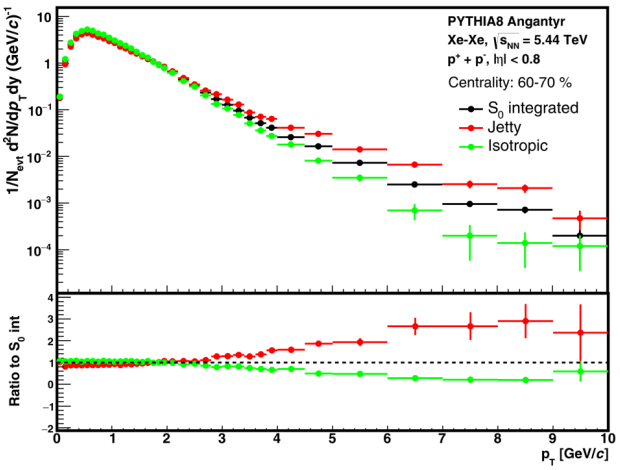

Fig. 19. p_T spectra of $p^{\pm}$ in the *centrality* bin 60–70% bin for PYTHIA

centrality (high-multiplicity) events and jettiness in high centrality (low-multiplicity) events in the charge particle production further suggests a reduction and the softening of the jet yields at high charged-particle multiplicities. Therefore, in the PYTHIA8 Angantyr model, where the high multiplicity events involve the large momentum transfer, the reduction in the jet contribution to the particle production may indicate a reduced production of back-to-back jets. Howe̅ver, we should keep in mind that the Angantyr does not include an assumption of a hot thermalized medium. Therefore, collective effects are absent in PYTHIA (Angantyr), whereas AMPT considers collective effects. From the Figs. 8 to 19, it is clearly visible that Pythia is clearly able to differentiate the ratio as compared to AMPT, where the ratio of jetty and isotropic p_T spectra with respect to the integrated S_0 move along the unity in the large p_T region. This indicates that the study of the jet production within PYTHIA8 Angantyr and AMPT will form an interesting subject.

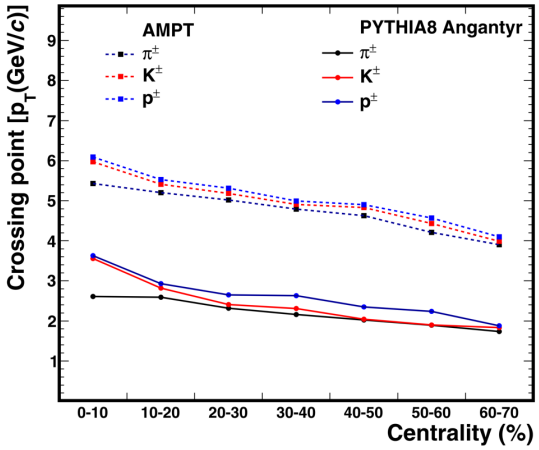

Fig. 20. The dependence of the *crossing point* on the centrality of the event for PYTHIA8 (filled circles) and AMPT (Square boxes), respectively

Table 3. **Table showing the *crossing point* (p_T in GeV/c) of jetty and isotropic events at mid-rapidity for Xe–Xe at $\sqrt{s_{NN}} = 5.44$ TeV collisions for PYTHIA8 and AMPT**

Centrality, %	$\pi^{\pm}$		$K^{\pm}$		$p^{\pm}$	
	PYTHIA	AMPT	PYTHIA	AMPT	PYTHIA	AMPT
0–10	2.61	5.83	3.56	5.97	3.63	6.09
10–20	2.59	5.2	2.82	5.41	2.93	5.53
20–30	2.32	5.02	2.41	5.18	2.65	5.31
30–40	2.16	4.79	2.31	4.91	2.63	4.99
40–50	2.02	4.63	2.04	4.83	2.35	4.90
50–60	1.89	4.21	1.90	4.43	2.24	4.57
60–70	1.73	3.9	1.83	3.99	1.88	4.1

4. Summary

In conclusion, using A Multi-Phase Transport Model (AMPT) and PYTHIA8 Angantyr one, we present the first application of the transverse spherocity analysis for Xe–Xe collisions at $\sqrt{s_{NN}} = 5.44$ TeV. The findings demonstrate that the transverse spherocity

successfully distinguishes between high-S_0 and low-S_0 heavy-ion collision event topologies. From the results, one can see that *crossing points* occur at relatively smaller p_T, as we go from low centrality to high centrality events. This means that, for low centrality events, the jettiness has a dominance over the isotropiness, whereas, for high centrality events, the isotropiness has dominance. For PYTHIA8 Angantyr, the *crossing point* occurs at much lower p_T as compared to AMPT indicating that the jet production occurs at much lower p_T for PYTHIA8 Angantyr as compared to AMPT. As we know, AMPT considers the formation of the medium and the collective effects, whereas PYTHIA8 Angantyr does not account for such happenings. Therefore, the jet production studies with both models will be of interest to do. The results, in our opinion, are extremely positive, and an experimental investigation in this direction would be very beneficial to comprehend the event topology dependence of the system dynamics in heavy-ion collisions.

1. A. Morsch [ALICE]. Multiple Parton Interactions with ALICE: from pp to p-Pb. *J. Phys. Conf. Ser.* **535**, 012012 (2014).
2. S. Chatrchyan *et al.* [CMS]. Jet and underlying event properties as a function of charged-particle multiplicity in proton–proton collisions at $\sqrt{s} = 7$ TeV. *Eur. Phys. J. C* **73** (12), 2674 (2013).
3. B. Abelev *et al.* [ALICE]. Transverse spherocity of primary charged particles in minimum bias proton-proton collisions at $\sqrt{s} = 0.9$, 2.76 and 7 TeV. *Eur. Phys. J. C* **72**, 2124 (2012).
4. S. Acharya *et al.* [ALICE]. Charged-particle production as a function of multiplicity and transverse spherocity in pp collisions at $\sqrt{s} = 5.02$ and 13 TeV. *Eur. Phys. J. C* **79** (10), 857 (2019).
5. J. Cleymans, D. Worku. Relativistic thermodynamics: Transverse momentum distributions in high-energy physics. *Eur. Phys. J. A* **48**, 160 (2012).
6. J. Cleymans, D. Worku. The Tsallis distribution in proton-proton collisions at $\sqrt{s} = 0.9$ TeV at the LHC. *J. Phys. G* **39**, 025006 (2012).
7. N. Mallick, R. Sahoo, S. Tripathy, A. Ortiz. Study of transverse spherocity and azimuthal anisotropy in Pb–Pb collisions at $\sqrt{s_{\rm NN}} = 5.02$ TeV using a multi-phase transport model. *J. Phys. G* **48** (4), 045104 (2021).
8. N. Mallick, S. Tripathy, A.N. Mishra, S. Deb, R. Sahoo. Estimation of impact parameter and transverse spherocity in heavy-ion collisions at the LHC energies using Machine learning. *Phys. Rev. D* **103** (9), 094031 (2021).
9. N. Mallick, S. Tripathy, R. Sahoo. Event topology and constituent-quark scaling of elliptic flow in heavy-ion collisions at the Large Hadron Collider using a multiphase transport model. *Eur. Phys. J. C* **82** (6), 524 (2022).
10. S. Prasad, N. Mallick, D. Behera, R. Sahoo, S. Tripathy. Event topology and global observables in heavy-ion collisions at the large hadron collider. *Sci. Rep.* **12** (1), 3917 (2022).
11. R. Rath, S. Tripathy, R. Sahoo, S. De, M. Younus, Identified particle production in Xe+Xe collisions at $\sqrt{s_{\rm NN}} =$ $= 5.44$ TeV using a multiphase transport model. *Phys. Rev. C* **99** (6), 064903 (2019).
12. J. Adam *et al.* [ALICE]. Centrality dependence of the nuclear modification factor of charged pions, kaons, and protons in Pb–Pb collisions at $\sqrt{s_{\rm NN}} = 2.76$ TeV. *Phys. Rev. C* **93** (3), 034913 (2016).
13. S. Acharya *et al.* [ALICE]. Transverse momentum spectra and nuclear modification factors of charged particles in pp, p-Pb and Pb-Pb collisions at the LHC. *JHEP* **11**, 013 (2018).
14. U. Heinz, R. Snellings. Collective flow and viscosity in relativistic heavy-ion collisions. *Ann. Rev. Nucl. Part. Sci.* **63**, 123 (2013).
15. Z. W. Lin, C. M. Ko, B. A. Li, B. Zhang, S. Pal. A Multiphase transport model for relativistic heavy ion collisions. *Phys. Rev. C* **72**, 064901 (2005).
16. C. Bierlich, G. Gustafson, L. Lönnblad, H. Shah. The angantyr model for heavy-ion collisions in PYTHIA8. *JHEP* **10**, 134 (2018).
17. B. Andersson, S. Mohanty, F. Soderberg. The Lund fragmentation process for a multigluon string according to the area law. *Eur. Phys. J. C* **21**, 631 (2001).
18. X. N. Wang. Role of multiple mini – jets in high-energy hadronic reactions. *Phys. Rev. D* **43**, 104 (1991).
19. X. N. Wang, M. Gyulassy. HIJING: A Monte Carlo model for multiple jet production in pp, pA and AA collisions. *Phys. Rev. D* **44**, 3501 (1991).
20. M. Gyulassy, X.N. Wang. HIJING 1.0: A Monte Carlo program for parton and particle production in high-energy hadronic and nuclear collisions. *Comput. Phys. Commun.* **83**, 307 (1994).
21. B. Zhang. ZPC 1.0.1: A Parton cascade for ultrarelativistic heavy ion collisions. *Comput. Phys. Commun.* **109**, 193 (1998).
22. V. Greco, C. M. Ko, P. Levai. Parton coalescence at RHIC. *Phys. Rev. C* **68**, 034904 (2003).
23. R.J. Fries, B. Muller, C. Nonaka, S.A. Bass. Hadronization in heavy ion collisions: Recombination and fragmentation of partons. *Phys. Rev. Lett.* **90**, 202303 (2003).
24. R.J. Fries, B. Muller, C. Nonaka, S.A. Bass. Hadron production in heavy ion collisions: Fragmentation and recombination from a dense parton phase. *Phys. Rev. C* **68**, 044902 (2003).
25. A. Khuntia, S. Tripathy, A. Bisht, R. Sahoo. Event shape engineering and multiplicity dependent study of identified particle production in proton + proton collisions at $\sqrt{s} =$ $= 13$ TeV using PYTHIA8. *J. Phys. G* **48** (3), 035102 (2021).

26. A. Ortiz, G. Paić, E. Cuautle. Mid-rapidity charged hadron transverse spherocity in pp collisions simulated with Pythia. *Nucl. Phys. A* **941**, 78 (2015).
27. S. Acharya *et al.* [ALICE]. Centrality and pseudorapidity dependence of the charged-particle multiplicity density in Xe–Xe collisions at $\sqrt{s_{\rm NN}} = 5.44$ TeV. *Phys. Lett. B* **790**, 35 (2019).
28. S. Tripathy, A. Bisht, R. Sahoo, A. Khuntia, M.P. Salvan. Event shape and multiplicity dependence of freeze-out scenario and system thermodynamics in proton+proton collisions at $\sqrt{s} = 13$ TeV using PYTHIA8. *Adv. High Energy Phys.* **2021**, 8822524 (2021).
29. A. Khatun, D. Thakur, S. Deb, R. Sahoo. J/ψ production dynamics: Event shape, multiplicity and rapidity dependence in proton + proton collisions at LHC energies using PYTHIA8. *J. Phys. G* **47** (5), 055110 (2020).
30. G. Bencédi [ALICE]. Event-shape- and multiplicity-dependent identified particle production in pp collisions at 13 TeV with ALICE at the LHC. *Nucl. Phys. A* **982**, 507 (2019).
31. S. Acharya *et al.* [ALICE]. Event-shape and multiplicity dependence of freeze-out radii in pp collisions at $\sqrt{s} =$ 7 TeV. *JHEP* **09**, 108 (2019).

Received 10.08.22

Р. Сінгх, Р. Бала, С.С. Самбял

АНАЛІЗ ПРОСТОРОВОГО РОЗПОДІЛУ ЗАРЯДЖЕНИХ ЧАСТИНОК, НАРОДЖЕНИХ У Xe–Xe ЗІТКНЕННЯХ ПРИ $\sqrt{s_{NN}} = 5{,}44$ TeB З ВИКОРИСТАННЯМ МОДЕЛІ PYTHIA8 ANGANTYR І БАГАТОФАЗНОЇ ТРАНСПОРТНОЇ МОДЕЛІ

Поперечна сферичність є змінною, яка дозволяє ефективно виокремлювати жорсткі та м'які компоненти процесів, що відповідають подіям із малою та великою кількістю партонних взаємодій, відповідно. Експериментальні дані, отримані нещодавно на прискорювачі LHC для малих систем, свідчать про важливість змінної поперечної сферичності для класифікації подій. В даній роботі ми вивчаємо динаміку генерації частинок у Xe–Xe зіткненнях при $\sqrt{s_{NN}} = 5{,}44$ TeB, використовуючи багатофазну транспортну модель і модель Angantyr, яка включена до PYTHIA8. Проаналізовано спектри поперечного імпульсу ідентифікованих частинок для м'яких (ізотропних) та жорстких (струминоподібних) подій в різних інтервалах центральності.

Ключові слова: кварк-глюонна плазма, псевдошвидкість, зіткнення важких іонів, багатофазна транспортна модель, PYTHIA8, модель Angantyr.